Javier Méndez Montejano

Final Master's Degree Project

Effect of Diabetes Mellitus conditions in cardiac organoids: an exploratory study

Directors: Josep Julve, Eder Fredy Mateus Medina

Group: Endocrine, Diabetes and Nutrition, and Pneumonology Research Groups, Research Institute Sant Pau, Barcelona, Spain

Master's Degree: Biochemistry, Molecular Biology, and Biomedicine program

Course: 2024/2025

University: Universitat Autònoma de Barcelona

ABSTRACT

Diabetes is a complex disease that is frequently linked to increased risk of different complications that shorten life quality and lifespan in affected subjects. The main characteristics of the disease are caused by metabolic derangements, particularly in carbohydrates and lipid management, due to impaired insulin signaling. In this context, diabetic cardiomyopathy (DCM) is a subclinical manifestation of cardiac disease that silently progresses in subjects with diabetes.

Organoid technology has upsurged in recent years, providing a powerful three-dimensional platform of human cardiomyocytes that structurally and functionally mimic human myocardium, enabling deeper insights into complex biological mechanisms. In this work, we aimed at setting up the culture conditions to develop cardiac organoids from iPSCs to explore the metabolic impact of diabetic mellitus (i.e., increased palmitic acid (PA), glucose, or both) in this setting. Our data showed that cardiac organoids expressed gene targets that are characteristics of myocardium. Gene expression analysis demonstrated the presence of ventricular and atrial markers, suggesting incipient cardiac modeling. Moreover, they exhibited a beating rate at baseline, as revealed by their spontaneous electrophysiological response and calcium transient amplitude. Interestingly, the exposure to voltage and beta-adrenergic stimuli in matured cardiac organoids compared to those at early stages of differentiation; however, such physiological behavior was not accompanied by concomitant changes in gene expression of structural and metabolic molecular targets. On the other hand, the exposition of cardiac organoids to increased glucose or PA concentrations did not modify the gene expression of cardiac-specific and metabolically-related molecular targets. In conclusion, we developed functional cardiac organoids *in vitro* to study cardiac remodelling and physiology. On the other hand, the established diabetic conditions did not lead to concomitant changes in the differential expression of molecular targets involved in carbohydrate and lipid metabolism.

Keywords: Diabetes Mellitus, diabetic cardiomyopathy, calcium handling, *in vitro* models, and cardiac organoids.

INDEX

LIST OF ABBREVIATIONS

- **18S:** 18S ribosomal RNA
- **2D:** Two-dimensional
- **3D:** Three-dimensional
- **ACTB:** Actin beta
- **AP:** action/potential
- **ATP2A2:** ATPase Sarcoplasmic/Endoplasmic Reticulum Ca2+ Transporting 2
- **AU:** Arbitrary units
- **BSA:** Bovine serum albumin
- **C:** Carbon
- **CD36:** Cluster of differentiation 36
- **cDNA:** complementary DNA
- **CMM1:** Complete maturation medium 1
- **CMM2:** Complete maturation medium 2
- **CPT1A:** Carnitine palmitoyltransferase 1A
- **Cq:** quantification cycle
- **DCM:** Diabetic cardiomyopathy
- **DKK2:** Dickkoft WNT signaling pathway inhibitor 2
- **DM:** Diabetes Mellitus
- **DMEM:** Dulbecco's Modified Eagle Medium
- **DNA:** Deoxyribonucleic acid
- **DPBS:** Dulbecco's Phosphate Buffered Saline
- **DSG:** Disaggregation of organoids
- **E8M:** Essential 8 medium
- **F/F_0:** normalized change in fluorescence intensity
- **FSC:** Forward Scatter Cell
- **G6PC:** Glucose-6- phosphatase catalytic subunit
- **GJA5:** Gap junction protein alpha 5
- **HG:** High glucose
- **hPSCs:** Human pluripotent stem cells
- **IGF-1:** Insulin-like growth factor-1
- **iPSCs:** Induced pluripotent stem cells
- **LPL:** Lipoprotein lipase
- **mRNA:** Messenger RNA
- **MYH7:** Myosin, heavy chain 7
- **MYL3:** Myosin light chain 3
- **NPPA:** Natriuretic peptide A
- **NPPB:** Natriuretic peptide B
- **PA:** Palmitic acid
- **PBS:** Phosphate-buffered Saline
- **PCK2:** Phosphoenolpyruvate carboxykinase 2, mitochondrial
- **qPCR:** Quantitative Polymerase Chain Reaction
- **RNA:** Ribonucleic acid

- **RNA e:** RNA extraction
- **RPMI:** Roswell Park Memorial Institute medium
- **SSC:** Side Scatter Cell
- **SEM:** Standard error of the mean
- **T1D:** Type 1 Diabetes Mellitus
- **T2D:** Type 2 Diabetes Mellitus
- **T3:** Triiodothyronine hormone
- **TNNT2:** Troponin T2, cardiac type
- **tto:** Treatment

INTRODUCTION

Diabetes Mellitus (DM) is a syndrome characterized by hyperglycemia and is classified into type 1 diabetes (T1D), type 2 diabetes (T2D), and some specific types, such as gestational diabetes. In T2D, there is a non-autoimmune heterogeneously progressive loss of functional islet β-cell insulin secretion in the presence of insulin resistance. There is a continuous hyperglycemia that could induce target organ damage, increasing the risk of panvascular atherosclerotic and macrovascular disease. Insulin resistance is considered a risk factor for the development of T2D, it is defined as the loss of the ability of target tissues to respond to insulin signals, resulting in hyperinsulinemia, associated with obesity and hypertension (Lu *et al.*, 2024). T2D accounts for 96% of diabetes; even with this high percentage, there is still no clear understanding of the pathogenesis *(ADA, 2024)*. It has become a worldwide problem because of its high prevalence, it is estimated to be the eighth leading cause of death combined with disability. In 2021, there were 529 million people of all ages in the world living with DM. There is an increase in the global age-standardized prevalence, ranging from 3.2% in 1990 to 6.1% in 2021 (Ong *et al.*, 2023; Vos *et al.*, 2020)).

Diabetic cardiomyopathy (DCM) is one of the main complications in individuals with DM in the absence of other cardiovascular diseases (Fan *et al.*, 2020). The risk of developing DCM increases in people with long-term diagnosed DM, poor glycemic control, and concomitant cardiovascular risk factors. DCM affects around 12-22% of T2D patients after 10 years of disease onset (Boudina and Abel, 2010). The pathophysiology of DCM is complex, but accumulating research suggests that its progression may be induced by metabolic derangements, particularly in carbohydrate and lipid management caused by impaired insulin signaling (Jia, Hill, and Sowers, 2018). As such, elevated glucose levels along with an excessive uptake of fatty acids, i.e., palmitic acid (PA) (C16:0), negatively influences cardiac remodeling and contractile function (Boudina and Abel, 2007), in a context of enhanced oxidative stress and inflammation (Stanley, Recchia and Lopaschuk, 2005).

For decades, the study of the metabolic processes and physiopathology of DCM has primarily been conducted in animal and *in vitro* models. In the case of animal models, there are significant differences in the substrate metabolism and cellular mechanisms that differ from those in humans (Kanisicak *et al.*, 2016). For instance, when comparing diabetic patients with mice under high-fat and high-sacarose diet, there is a difference in cardiac efficiency, which is lower in diabetic patients, but it remains without any changes in the mice-group; the size of the heart increases while the contractile function decreases in diabetic patients, while there is almost no statistically significance in the murine model. Finally, there was no difference in

oxidative stress in Zucker mice, while this parameter is usually increased in diabetic patients (Riehle and Bauersachs, 2019).

In contrast, the use of two-dimensional (2D) cell cultures represents an approach for investigating disorders where preclinical animal models are insufficient or lack adequate predictive validity; they offer several benefits, including simple and easier paths to conduct molecular, biological, and metabolic experiments. However, 2D cultures systems present some limitations: the monolayer lacks complex structure and multi-cellular organization; they do not have crosstalk between different cells types; cell maturity is low; the contractile force records of individual cells vary greatly; they can only be used to detect direct effects of drugs on cardiomyocytes and the systemic effect cannot be evaluated (Weinberger, Mannhardt and Eschenhagen, 2017); (Nugraha, Buono and Emmert, 2018); (Evans and Kaufman, 1981).

In the recent few years, the use of induced pluripotent stem cells (iPSC), which are generated by induced reprogramming of somatic cells through the forced expression of transcription factors, offer a valuable utility in recreating tissue modeling and deepening into the metabolic basis of different diseases (Volpato and Webber, 2020), mainly due to due their self-renewal and differentiation capabilities (Mattapally *et al.*, 2018). Specifically, three-dimensional (3D) organoids are used to generate human “disease-in-a-dish” models, by the ability of human iPSCs to self-organize as sphere-shaped mini-organs that under disease-specific conditions may exhibit similar functional properties as those seen *in vivo* (Jo *et al.*, 2016); (Mattapally *et al.*, 2018). This system is commonly established by suspension culture to avoid direct physical contact with the dish, which is generally achieved using scaffold or scaffold-free techniques. The first one can be done with the use of Matrigel, a heterogeneous and gelatinous protein mixture secreted by mouse sarcoma cells. For scaffolding-free techniques, cells are hanging in a medium from a plate by gravity and surface tension. Alternatively, the organoids can also be established via “air-liquid-interphase”, here, cells are first cultured submerged in medium, on a basal layer of fibroblasts, then, it gradually evaporates and the upper cell layers are exposed to the air, to allow polarization and differentiation (Corrò, Novellasdemunt and Li, 2020).

Cardiac organoids can be achieved using different laboratory protocols. In this context, the development of cardiac organoids based on iPSCs-derived cardiac cells allows a specific control over cell type ratios and the functional study of disease-causing mutations in a particular cell type (Liu *et al.*, 2022). Since heart tissue is composed of different cell types, mainly of cardiomyocytes, as well as cardiac endothelial cells and cardiac fibroblasts. (Jo *et al.*, 2016), cardiac organoids technology has been used to study the embryonic heart structure and spatial-temporal patterning during early cardiogenesis (Drakhlis *et al.*, 2021). Therefore, cardiac organoids are ideal for studying human developmental heart

diseases, e.g., cardiac malformations and regeneration after injury (Hofbauer *et al.*, 2021). Additionally, cardiac organoids accurately mimic the physiological and pathological conditions of the human heart with precision and advanced cellular maturity stages. Despite this, the complex cell system is far from perfect and still presents various limitations; it consistently falls short in recapitulating essential aspects of human heart development, such as anterior-posterior patterning and coronary vascularization, among others (Volmert *et al.*, 2023).

Herein, we report a set of optimized conditions for inducing the development of human heart organoids to assess their structure and functionality. To replicate human DCM *in vitro*, human pluripotent stem cells (hPSC)-derived cardiomyocytes were exposed to chronic hyperglycemic stress, which has been previously described to induce pathological hypertrophy and reduced contractility (Ng *et al.*, 2018). Furthermore, we also assessed the potential role of increasing free fatty acids (i.e., PA), another metabolic hallmark of defective insulin signaling, to assess their impact on cardiac remodeling and physiology.

OBJECTIVES

1. To set up *in vitro* conditions to obtain cardiac organoids derived from iPSCs. The operative objectives were:

   [i] To assess functional (i.e., measuring the voltage and calcium-related beating pulses) differences between early (10 days) and mature stages (40 days) of differentiation under basal (i.e., spontaneous) and after (a) external electrical stimuli or (b) incubation of a β-agonist (isoproterenol).

   [ii] To assess the gene expression of molecular targets of cardiac physiology and remodeling in both differentiation stages as indicated above.

2. To assess the impact of diabetic conditions, mimicked by the chronic (one week) exposure of matured cardiac organoids (40 days) to elevated concentrations of palmitic acid, glucose, or both, on the cellular characteristics (using cytometric analysis) and molecular profile (using real time qPCR analysis).

METHODS

For the generation of self-organizing patterned human heart organoids, a protocol describing the different steps from developmental induction was followed (Volmert and Aguirre, 2024). Human iPSC (SCTi003-A StemCell) were used for this study. Division capacity and differentiation were tested daily in the development of the cells.

Induced Pluripotent Stem Cell (iPSCs) cultures

Cell thawing

To thaw iPSCs, cells were collected from the nitrogen chamber and placed in warm water at 37º C for 2 minutes. Cells were collected and transferred into a tube, then 8 mL of DMEM-18 (Dulbecco's Modified Eagle Medium) (Gibco, USA) were added. Then, the tube was centrifuged at 120 g for 3 minutes, supernatant was aspirated and 2 mL of E8M (Essential 8 Flex medium (Gibco, USA), Essential 8 Supplement at 50X (Gibco, USA) and 1% of penicillin-streptomycin) with 10 mM of Thiazovivin (ROCK inhibitor) (Sigma-Aldrich Netherlands)) were added to resuspend iPSCs. Cells were plated in one well of a six-well Matrigel-coated plate and placed in a sterile incubator at 37 ºC and 5% CO_2 for 24 hours. Once the cells reached 70% confluency, they were either expanded or processed for cardiac organoid generation. For iPSCs expansion, cells were washed with 1X DPBS (Dulbecco's Phosphate Buffered Saline) (Gibco, USA) using 1 mL of ReLeSR™ (StemCell, Canada), after 6 minutes of acting on the cells the reaction was stopped with 1 ml of E8M, and the cells were detached from the plate.

Self-assembling human heart organoid differentiation

On day -2 (*embryoid body formation.* **Figure 1**), for cardiac organoid generations, once the iPSCss reached 70% confluency, cells were washed with 1X DPBS (Gibco, USA) and dissociated with Accutase (Innovative Cell Technologies, USA) for five minutes to get a single-cell suspension. iPSCs were collected in 15 mL tubes and centrifuged at 120 g for 3 minutes. Cells were resuspended in E8M with 10 mM of Thiazovivin, and cell number and viability were determined using a Corning cell counter. Then, cells were resuspended in E8M with 10 mM of Thiazovivin to achieve a density of 1 × 10^5 cells/mL, and 100 µL/well were seeded on a round-bottom 96-well ultra-low attachment plate. The plate was centrifuged at 100 g for 3 minutes and then placed in a sterile incubator at 37 ºC with 5% CO_2 for 24 hours. **On day -1,** 50 µL of each well were removed and 200 µL of E8M were added. The plate was placed inside the incubator for an additional 24 hours. **On day 0** (*mesoderm induction*), 166 µL of medium were removed from each well, and 166 mL of **RPMIB** (Rosewell Park Memorial Institute) (RPMI/B27 minus insulin (Gibco, USA); 1% penicillin/streptomycin) **+3 medium** (6 mM CHIR99012 (Sigma-Aldrich USA); 36 pM BMP4 (Gibco, USA) and 8 pM Activin A (Gibco, USA)) were added, then the plate

was placed inside the sterile incubator. **On day 1**, 166 µL of medium was removed from each well and replaced with 166 µL of **RPMIB** (RPMI/B27 minus insulin; 1% penicillin/streptomycin). On day 2 (*cardiac mesoderm induction*), 166 mL of medium were removed from each well, and 166 mL of **RPMIB+W** (RPMI/B27 minus insulin; 3 mM Wnt-C59 (Selleck, USA)) were added; finally, the plate was incubated for 48 hours. **On day 4**, 166 µL were removed and replaced with 166 µL of RPMIB and then the plate was incubated for 48 hours. **On day 6**, 166 mL was removed and replaced with 166 µL of **RPMIB+I** (RPMI with B27 supplemented with insulin (Gibco, USA); 1% penicillin/streptomycin (Gibco, USA)), then incubated for 24 hours. **On day 7** (*epicardial induction*), 166 µL was removed and replaced with 166 µL of RPMIB+C (RPMI with B27 supplemented with insulin; 1% penicillin/streptomycin and 4 mM CHIR99012 (Sigma-Aldrich, USA), the plate was incubated for 1 hour and then 166 µL were removed and replaced with 166 uL of RPMIB+I, then it was incubated for 48 hours. From **days 9 to 21** (*growth and maintenance*), the media was changed every 48 hours, removing 166 µL and adding 166 µL of RPMIB+I. At this point, an observational assessment of organoids' structure and contractile activity was done. The scaling bar used in photographs was obtained using ImageJ Software.

Development of conditions for maturation induction

By **day 23** (grown stage), organoids were put into developmental maturation conditions as follows: from **day 23 to 29**, the first half maturation process was done, performing media changes every 48 hours with the complete maturation medium 1 (CMM1) (containing stock 50X RPMI/B27 (Gibco, USA), 1% penicillin streptomycin (Gibco, USA)), 0.4 mM ascorbic acid (Merck, Germany); 4 mM glucose (Gibco USA); 54.4 µM palmitate BSA (Bovine Serum Albumin) (Sigma-Aldrich, USA); 40.5 µM oleate BSA (Sigma-Aldrich USA); 22.5 µM linolate BSA (Sigma-Aldrich, USA); 120 µM L- carnitine (Sigma-Aldrich, USA); 30 nM T3 hormone (Sigma-Aldrich USA) and 50 ng/mL IGF-1 (Insulin-like growth factor-1) (PeproTech, USA)). From **days 29 to 35**, in the second half of the maturation process, the media of cardiac organoids was changed every 48 hours, using complete maturation medium 2 (CMM2) (CMM1 without IGF-1).

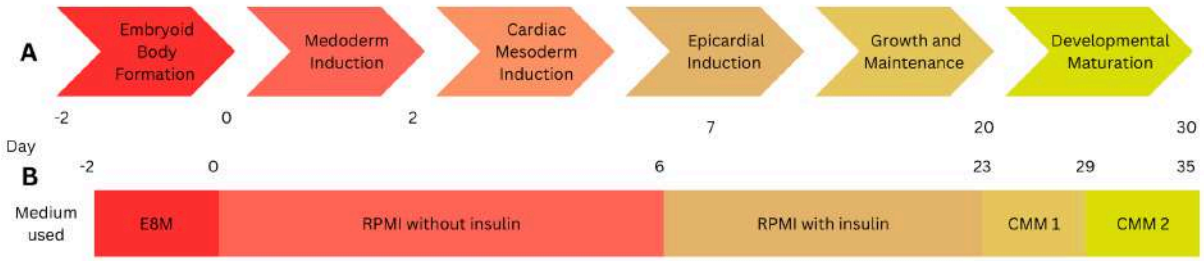

Figure 1. Timeline of developmental periods in cardiac organoids. A. Description of the different growing and developmental periods of heart organoids. **B.** Protocol depicting the major media changes and timepoints, compared to the developmental stages.

Diabetic state induction

Compound treatments

The diverse compound treatments were developed using a protocol that explained the generation of diabetic conditions within cardiac organoids (Volmert *et al.,* 2023). The experiment was conducted using four distinct batches of cardiac organoids. These groups were systematically distributed across a 96-well ultra-low attachment plate, with each row specifically allocated to a different experimental group, each composed of 10 cardiac organoids. From **day 35** (once achieved matured stage) **to 41**, the medium mimicking diabetic conditions were administered every 48 hours, we had 6 groups (**Figure 2**), as follows: **1)** Carrier group: 50x RPMI/B27, 1% penicillin streptomycin, 0.4 mM ascorbic acid, 40.5 mM oleate BSA, 22.5 mM linoleate BSA, 120 mM L-carnitine, 30 nM T3 hormone, 4 mM glucose and 11% BSA (Sigma-Aldrich, USA). **2)** Control group: 50x RPMI/B27, 1% penicillin streptomycin, 0.4 mM ascorbic acid, 40.5 mM oleate BSA, 22.5 mM linoleate BSA, 120 mM L-carnitine, 30 nM T3 hormone, 4 mM glucose, and 52.5 µM palmitic acid. **3)** Increased palmitic acid group (2.25 mM): 50x RPMI/B27, 1% penicillin streptomycin, 0.4 mM ascorbic acid, 40.5 mM oleate BSA, 22.5 mM linoleate BSA, 120 mM L-carnitine, 30 nM T3 hormone, 4 mM glucose, and 2.25 mM palmitic acid. **4)** Increased palmitic acid group (10 mM): 50x RPMI/B27, 1% penicillin streptomycin, 0.4 mM ascorbic acid, 40.5 mM oleate BSA, 22.5 mM linoleate BSA, 120 mM L-carnitine, 30 nM T3 hormone, 4 mM glucose, and 10 mM palmitic acid. **5)** Increased glucose group: 50x RPMI/B27, 1% penicillin streptomycin, 0.4 mM ascorbic acid, 40.5 mM oleate BSA, 22.5 mM linoleate BSA, 120 mM L-carnitine, 30 nM T3 hormone, 1.1 M glucose, and 52.5 µM palmitic acid. **6)** Increased glucose and palmitate group: 50x RPMI/B27, 1% penicillin streptomycin, 0.4 mM ascorbic acid, 40.5 mM oleate BSA, 22.5 mM linoleate BSA, 120 mM L-carnitine, 30 nM T3 hormone, 1.1 M glucose, and 2.25 mM palmitic acid. At this point, an observational assessment of organoids' structure and contractile activity was done. The scaling bar used in photographs was obtained using ImageJ Software.

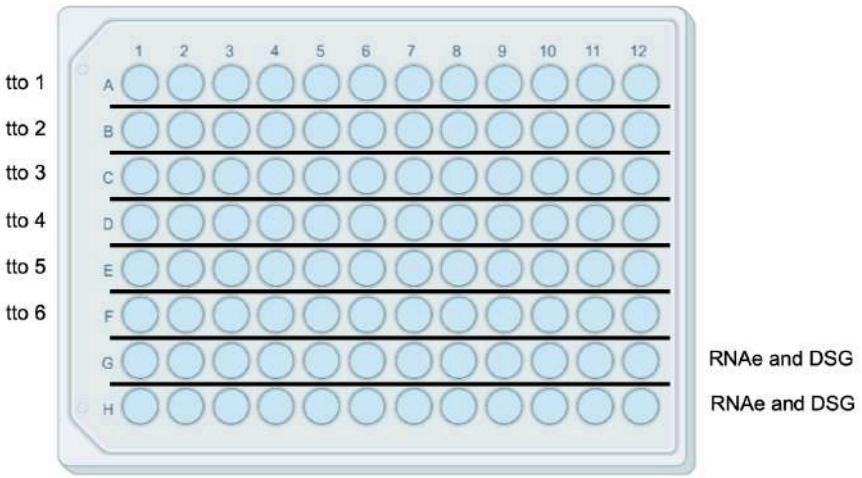

Figure 2. Distribution of different compound treatments and techniques performed in the round-bottom 96-well ultra-low attachment plates. Carrier (tto 1), in this row, the compound did not include glucose or palmitic acid. Control group (tto 2), here the composition of the medium was the same as the CMM (Complete maturation medium) without IGF-1. Increased concentration of palmitic acid (tto 3) (2.25 mM). Highest concentration of palmitic acid (tto 4) (10 mM). Increase in glucose (tto 5) (1.1 M). Increase in glucose (1.1 M) and palmitic acid (2.25 mM) (tto 6). In rows "G" and "H", the organoids were maintained in the control medium and used for RNA extraction (RNAe) and disaggregation (DSG). Abbreviations: tto: treatment.

Gene expression analysis

RNA extraction

Organoids were collected during each developmental periods: before starting the maturation period in day 23 (a total of three organoids), before starting the diabetic conditions in each group in on day 35 (a total of three organoids) and after finishing the diabetic mimicking period on day 41 (three organoids per group) (**Figure 3**). Once all the samples were collected in the respective Eppendorfs, they were centrifuged for 20 seconds at 13000 rpm. The supernatant was removed with a pipette and discarded. Then, 1 mL of DPBS was added to each Eppendorf tube to wash the pellet, and the tubes were centrifuged again.

To perform RNA extraction, a commercial Omega Bio-tek E.Z.N.A.® Total RNA Kit I was used following the manufacturer's recommended protocol as described below.

Once centrifugation was complete, the supernatant was removed and 350 µL of TRK lysis buffer (Lot. 43360GF76) were added. Cardiac organoids were completely lysed by pipetting movements (up and down). Then, 350 µL of 70% ethanol were added to the mixture, and the suspension was homogenized by pipetting. The 700 µL were transferred to HiBind® RNA Mini Columns (Lot. 32586CL96) on 2 mL Collection Tube (Lot. 41146G421). The column was centrifuged, and the supernatant was discarded.

After that, 500 µL of wash buffer I (Lot. 35672EZ77) were added, centrifuged for 2 minutes at 10,000 rpm, and the supernatant was discarded. Then, 500 µL of wash buffer II (Lot. 40794FA57) were added, centrifuged under the conditions mentioned above, and then the liquid was discarded again. This step with wash buffer II (Lot. 40794FA57) was repeated once more.

Once the washes were completed, the column was centrifuged at maximum speed for 2 minutes to ensure that it was completely dry. Finally, the column was transferred to a new 2 mL Eppendorf and 40 µL of nuclease-free water (Lot. 43919DZ75) were added to the column to dilute the genetic material. The column was centrifuged at maximum speed for 2 minutes to recover the RNA. Samples were stored at -80ºC until further analysis.

RNA quantification

The RNA quantification was performed using the Nanodrop 2000 Spectrophotometer (Thermo Scientific). The values were retrieved using the Nanodrop 2000 software using 1.5 µL of each sample and were performed during 3 major phases in the development of the cardiac organoids (**Figure 3**).

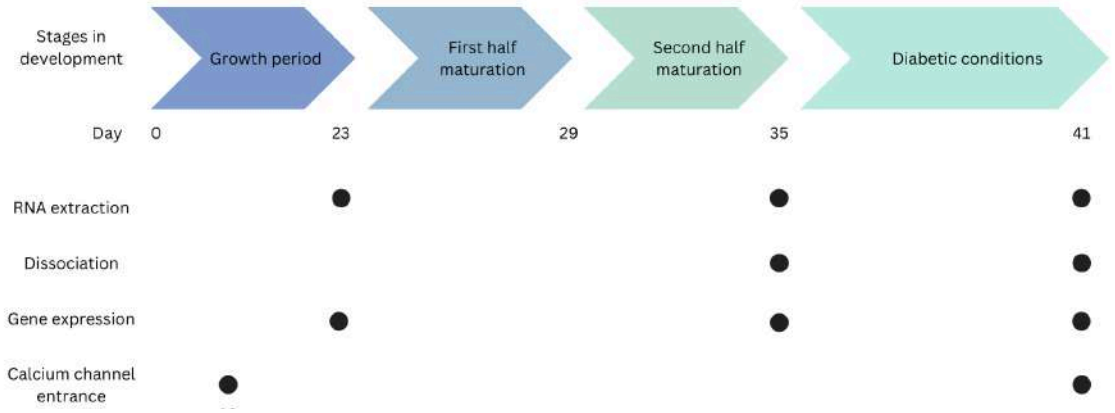

Figure 3. Sampling process performed during differentiation periods. Schematic representation of the timeline used for the different batches (*n*=4) of cardiac organoids. The methods performed were RNA extraction, dissociation to obtain cell size and granularity, gene expression and calcium channel entrance to measure spontaneous and induced electrical activity on organoids (*n*=2), the first one at 10-days of age and the second one at 40-days of age.

Gene expression assay

To determine the spatial specificity of gene expression within the cardiac organoids, a panel of predesigned validated primers (TaqMan probes (Life Technologies, USA) of molecular targets was used. The molecular targets included ventricular markers: *MYH7* and *MYL3*; atrial markers: *NPPA* and *GJA5*; valvular structures: *DKK2*; cardiac-specific troponin: *TNNT2*. (Volmert *et al.,* 2023). To assess lipidic metabolism: *CD36*; carbohydrate metabolism: *G6PC*; glycosidic metabolism: *PCK2*; natriuretic peptide: *NPPB*; calcium entry and exit limiting protein: *ATP2A2*; beta oxidation of mitochondrial fatty acids: *CPT1A*; lipolysis: *LPL* and housekeeping: *ACTB* and *18S* (**Table 1**).

A protocol described by Méndez-Lara et al., (2018) was used as a reference to perform this technique. Quantitative real-time RT-PCR analysis description: Total mRNA (1 µg) was reverse-transcribed with random primers using M-MLV Reverse Transcriptase, RNase H Minus, and Point Mutant (Promega, USA) to generate cDNA.

Real-time PCR assays were performed on a C1000 Thermal Cycler coupled to a thermal cycler device (Bio-Rad Laboratories, Spain). All analyses were performed in duplicate. *ACTB* was used as a housekeeping gene, whereas *18S* was used to

normalize the mRNA levels. The relative mRNA expression levels were calculated using the ΔΔCt method.

Table 1. List of selected Taqman probes used.

Gene name	Assay ID	Catalog number	Supplier
MYH7	Hs01110632_m1	4453320	ThermoFisher USA
MYL3	Hs00264820_m1	4448892	ThermoFisher USA
NPPA	Hs00383231_m1	4453320	ThermoFisher USA
GJA5	Hs00979198_m1	4448892	ThermoFisher USA
DKK2	Hs00205294_m1	4448892	ThermoFisher USA
TNNT2	Hs00943911_m1	4453320	ThermoFisher USA
PCK2	Hs00388934_m1	4453320	ThermoFisher USA
G6PC	Hs02802676_m1	4448892	ThermoFisher USA
ATP2A2	Hs01564013_m1	4448892	ThermoFisher USA
CPT1A	Hs00912671_m1	4453320	ThermoFisher USA
NPPB	Hs00173590_m1	4453320	ThermoFisher USA
CD36	Hs00169627_m1	4453320	ThermoFisher USA
LPL	Hs00173425_m1	4453320	ThermoFisher USA
ACTB	Hs01060665_g1	4453320	ThermoFisher USA
18S	Hs03003631_g1	4453320	ThermoFisher USA

Electrical activity of cardiac organoids

To visualize changes in the membrane potential and the intracellular calcium concentration, cardiac organoids on days 10 and 40 of maturation were loaded with Fluovolt™ using the Membrane Potential Kit (Invitrogen, USA) and 5 mM Rhod-2 AM (Invitrogen, USA), respectively. First, a suspension including 332 µl of RPMI/B27 and 5 mM Rhod-2 AM was prepared. In a separate tube, a second suspension was prepared by adding 5 µl of PowerLoad Concentrate and 0.5 µl of Fluovolt™ Dye. The two suspensions were homogeneously combined, and subsequently, 166 µl from each well was extracted and replaced with 166 µl of the medium containing the dyes. The plate was then placed inside the incubator for one hour. After one hour, the medium was replaced with 166 µL of RPMI/B27 in each well, and the organoids were placed in a FluoroDish™ (FD3510-100, WPI) for further analysis using a confocal microscope. To perform the experiments, the solution was switched to

oxygenated physiological buffer at 37ºC containing (in mM): 132 NaCl, 4 KCl, 4 NaHCO3, 0.33 NaH2PO4, 2 CaCl2, 1.6 MgCl2, 10 HEPES, 5 glucose, 5 sodium pyruvate with 5 mM Mavacamten to prevent contractions and avoid motion artifacts. The experiments were performed under control conditions and after 10 minutes of incubation with the beta-adrenergic agonist isoproterenol (100 nM) to assess its effect on the calcium transient amplitude and frequency in the organoids. Confocal voltage and calcium images (512 x 512 pixels) were recorded at a frame rate of 90 Hz, using a resonance-scanning confocal microscope with a 10x glycerol-immersion objective (Leica SP5 AOBS, Wetzlar, Germany). Induced electrical activity was measured using external electrodes at a rate of 0.5, 1, and 2 Hz. Representative images and traces were obtained from the data files using the LAS AF Lite software (Leica Microsystems, Wetzlar, Germany).

Organoid dissociation to single cell suspension

The dissociation of cardiac organoids was accomplished using STEMdiff™ Cardiomyocyte Support Medium (Stemcell Technologies, Canada) and STEMdiff™ Cardiomyocyte Dissociation Medium (Stemcell Technologies, Canada). The STEMdiff™ Cardiomyocyte Dissociation Medium was placed in a water bath at 37ºC and the STEMdiff™ Cardiomyocyte Support Medium was left at ambient temperature. First, the desired amount of organoids were put on a 1.5 mL Eppendorf, then the medium transferred into a different Eppendorf to keep the sample in -80ºC for storage; then, 1 mL of PBS was added to each Eppendorf with the organoids, then, the PBS was discarded and 300 µL of STEMdiff™ Cardiomyocyte Dissociation Medium were added. The Eppendorf tubes were placed in a Thermomixer comfort for 5 minutes at 37 °C and 300 rpm. During the 5 minutes, 3 mL of STEMdiff™ Cardiomyocyte Support Medium were added on a 15 mL Falcon tube; once the 5 minutes were over, the the sample from the Eppendorf was moved up and down with a pipette, then the 300 µL were transferred into the 15 mL Falcon tube, this step was performed 2 more times until 900 µL of STEMdiff™ Cardiomyocyte Dissociation Medium in total were added into the 15 mL Falcon tube. The content of the 15 mL tube was filtered and then transferred into a new 15 mL Falcon tube for further analysis.

Flow cytometry analysis

Following organoid dissociation into single cell suspension from each compound group, 100 µL of the suspension were collected and transferred into a 5 mL Falcon tube where it was centrifuged at 300 g for 5 minutes, after this, the supernatant was discarded, then washed with 100 µL of 1x phosphate-buffered saline (PBS) (Gibco, USA) into each 5 mL Falcon tube, it was centrifuged at 300 g for 5 minutes and the supernatant was discarded, finally, cells were fixed using 100 µL of PBS 4%

paraformaldehyde to each 5 mL Falcon tube and was stored in -4ºC for further analysis.

Statistical analysis

The data are expressed as the mean ± standard error of the mean (SEM). The effects of treatment on levels of gene expression were determined using parametric one-way ANOVA followed by a Tukey post test. The relationship between variables was tested with Pearson's correlation. The comparison between organoids after finishing the growth and matured stage was determined using a non-parametric test, in this case, Mann-Whitney U test. Statistical analyses were performed using GraphPad Prism software (GPAD, version 5.0, San Diego, CA, USA). A *p-value* < 0.05 was considered to define significant differences.

RESULTS

Cardiac organoid development: comparison of early and late stages

Gross anatomical structure and function

Photographic documentation throughout cardiac organoid development revealed different morphological and functional characteristics at different time points. In our observations, the percentage of beating cardiac organoids reached around 90%. A 16 day-old organoid displayed a defined structure with localized beating, while a mature 40 day-old organoid presented a more spherical morphology and a sequential beating pattern, starting in the upper region and followed by a secondary contraction in the lower region, mimicking human cardiac rhythm (**Figure 4**).

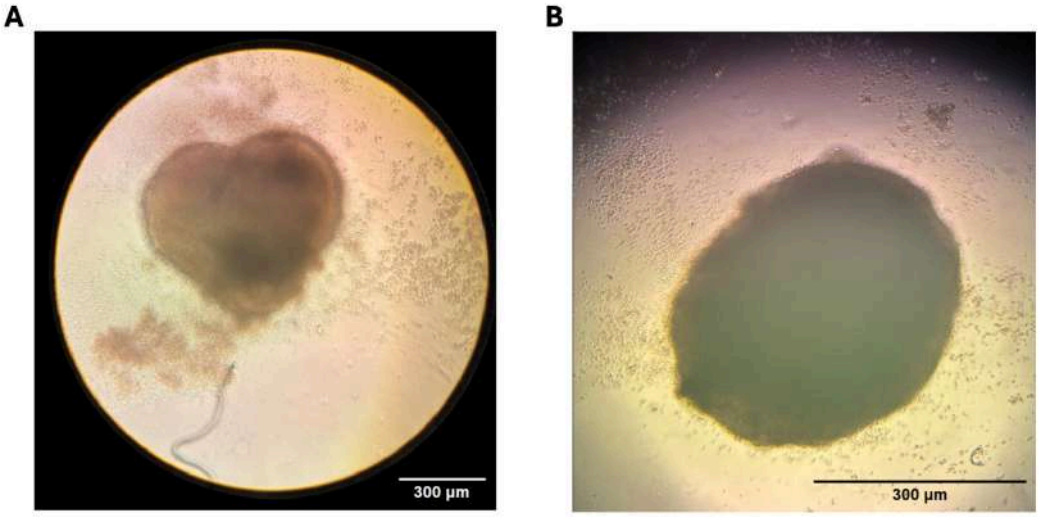

Figure 4. Photographs of the gross structure of cardiac organoids. **A)** Immature organoid at 16 days of development seen at an optical microscope with a 4x lens. **B)** Matured organoid at 40 days of development, seen at an optical microscope with a 10x lens. Scale set at 300 µm.

Gene expression analysis

Developmental stages comparison

Analysis of gene expression of different molecular markers revealed no statistically significant differences across groups. This observation applies to genes associated with metabolic pathways as well as those encoding proteins for anatomical structures. Cq presented an expression over the different compound groups with values ranging from 23 to 30 (**Figure 5**).

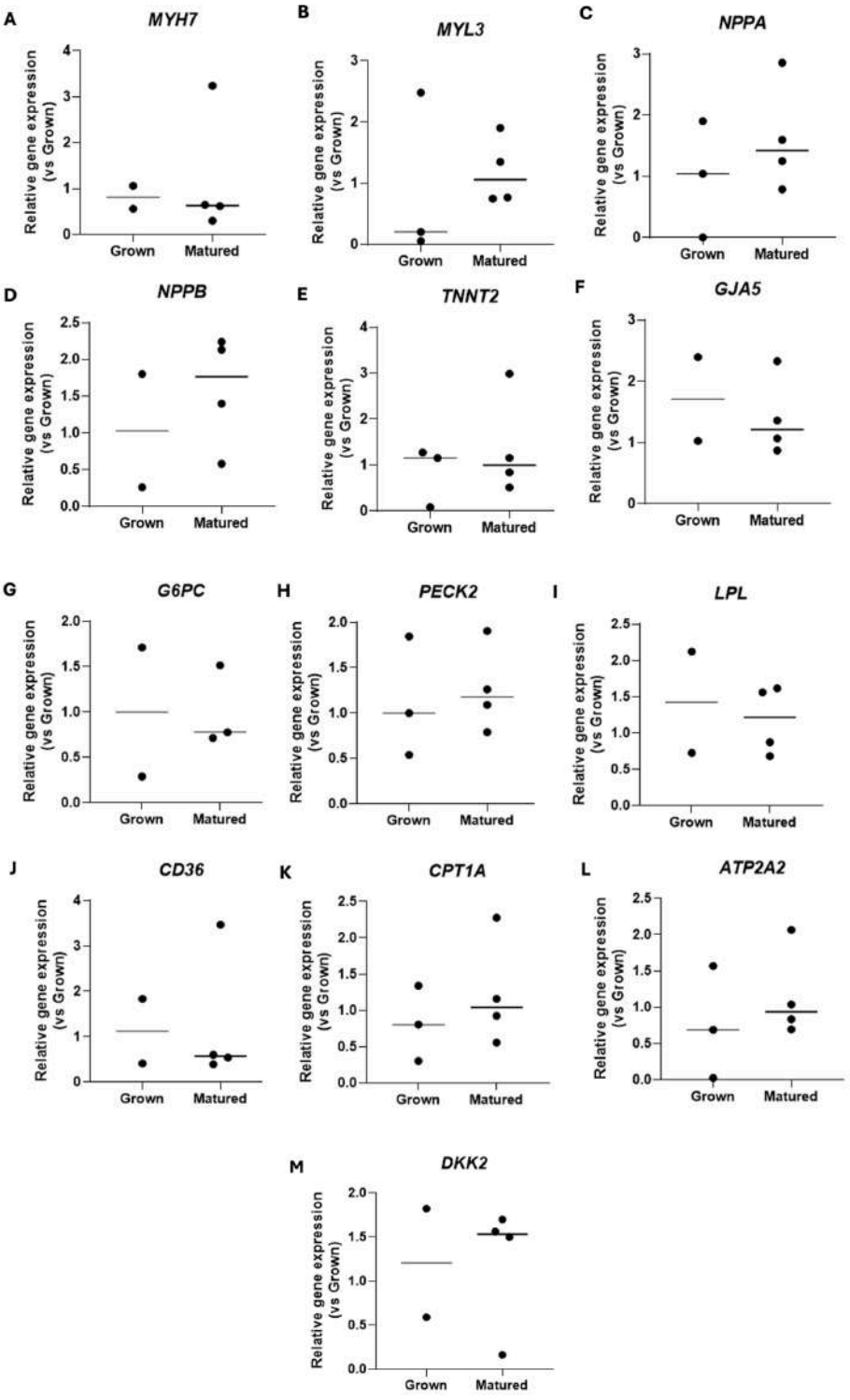

Figure 5. Gene expression in two different developmental stages. Graphical representation of gene expression comparing cardiac organoids in two different developmental stages, "grown" corresponds to the organoid when the grown conditions were achieved at day 23 and "matured" corresponds to the cardiac organoids when the maturation process was completed at day 35 (*n*= 2-4 organoids from each batch). Relative gene expression of: **A)** *MYH7* (Cq= 29.0), **B)** *MYL3* (Cq= 24.5), **C)** *NPPA* (Cq= 23.9), **D)** *NPPB* (Cq= 29.7), **E)** *TNNT2* (Cq= 23.6), **F)** *GJA5* (Cq= 27.7), **G)** *G6PC* (Cq= 29.7), **H)** *PECK2* (Cq= 29.2), **I)** *LPL* (Cq= 29.1), **J)** *CD36* (Cq= 29.4), **K)** *CPT1A* (Cp= 28.9), **L)** *ATP2A2* (Cq= 23.2) and **M)** *DKK2* (Cq= 30.2). Abbreviations: Cq: quantification cycle. HG: high glucose. PA: palmitic acid. tto: treatment.

Electrical activity of cardiac organoids

Voltage and Calcium channel entrance activity

Spontaneous electrophysiological response and calcium transient amplitude were assessed. Our analysis revealed a concurrent peak in both variables during the same timeframe (**Figure 6**), indicating a strong correlation where electrical activity appears to be a consequence of calcium signaling. Furthermore, a comparison between day 10 and day 40 organoids demonstrated significant improvements in maturation. We observed an increase in beating activity and a more stable rhythm in the matured organoid (day 40). Simultaneously, calcium peaks were notably higher in these late stage organoids compared to their earlier stage counterparts. Finally, isoproterenol stimulation resulted in an increased beating rate in day 40 organoids; nonetheless, this effect was less pronounced in day 10 organoids.

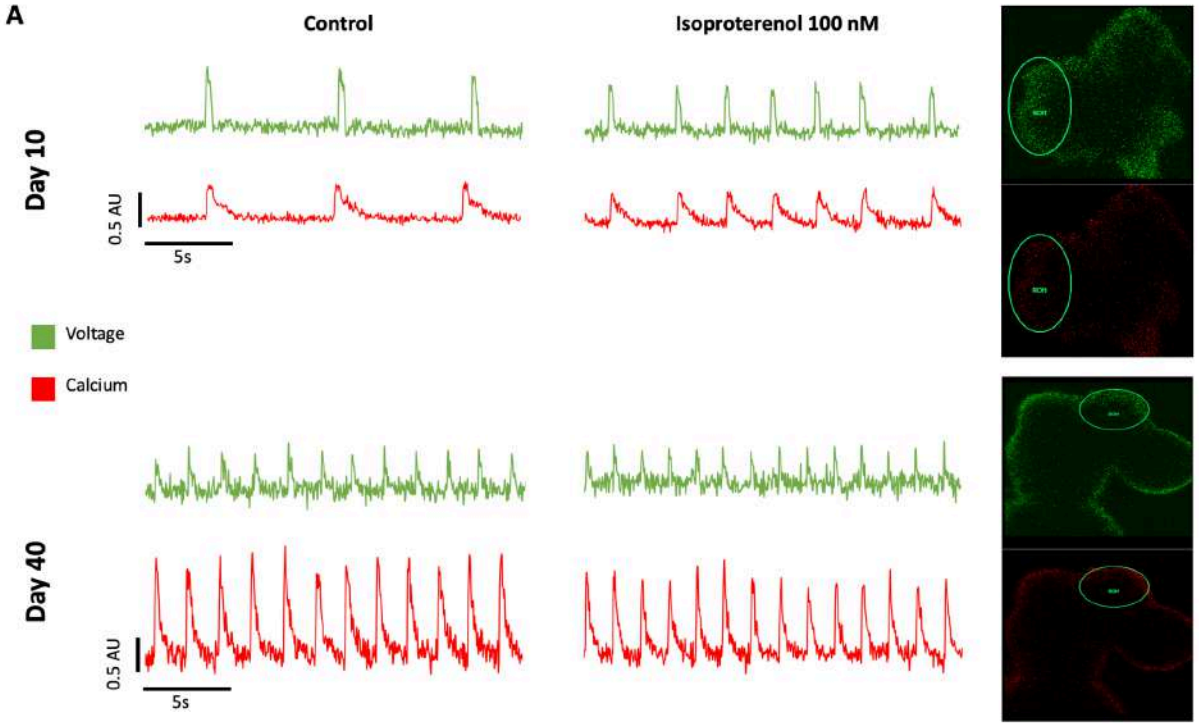

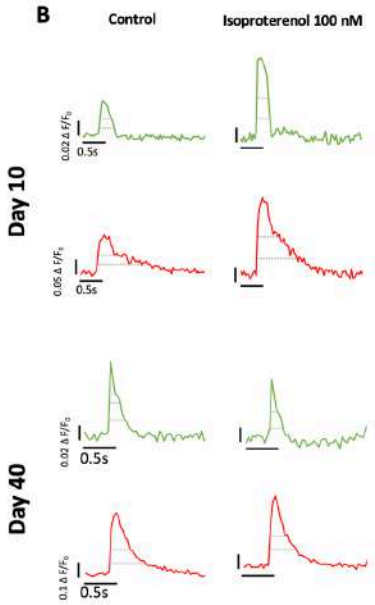

C

Control							
Day 10				Day 40			
Voltage		Calcium		Voltage		Calcium	
50%	75%	50%	75%	50%	75%	50%	75%
0.29 s	0.33 s	0.37 s	0.96 s	0.16 s	0.22 s	0.31 s	0.55 s
Isoproterenol 100 nM							
Day 10				Day 40			
Voltage		Calcium		Voltage		Calcium	
50%	75%	50%	75%	50%	75%	50%	75%
0.22 s	0.29 s	0.44 s	0.83 s	0.12 s	0.18 s	0.24 s	0.39 s

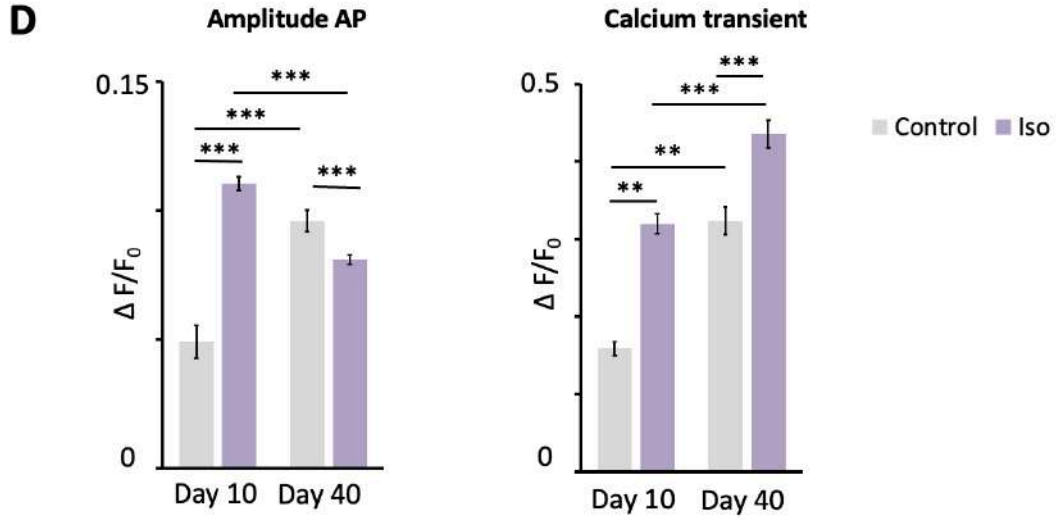

Figure 6. Spontaneous and induced electrical activity from a 10 and 40 day-old cardiac organoid. A) Comparison of voltage and calcium entrance activity between 10 and 40 day-old cardiac organoids (*n*=2) within a region of interest (ROI). First, it was measured with a control group (images on the left) and then by applying 100 nM isoproterenol (β-agonist) (images on the right). **B)** Mean voltage and calcium entrance activity of the different peaks of action potential in the 10 and 40 days-old organoids. The times of 50 and 75% of activity inside the curve were measured (dotted gray lines). **C)** Table of the time it took to reach 50 and 75% of the activity inside the curve from the mean peak of the different voltage and calcium entrance peaks. **D)** Histograms comparing the amplitude of action potential (AP) vs. F/F_0 of control and 100 mM isoproterenol groups of 10 and 40 days-old cardiac organoids (left) and calcium transient vs. F/F_0 of control and 100 mM isoproterenol groups of 10 and 40 days-old organoids (right). Abbreviations: AU: arbitrary units. F/F_0: normalized change in fluorescence intensity. Iso: isoproterenol. ROI: region of interest. S: seconds. * $P \leq 0.05$, ** $P \leq 0.01$ and *** $P \leq 0.001$ vs either baseline or early stage conditions, as appropriate.

External electrical activity

External electrical stimuli were applied at frequencies of 0.5 Hz, 1 Hz, and 2 Hz to cardiac organoids aged 10 and 40 days. A noticeable difference emerged in the 2 Hz stimulation group where the 10 day-old organoid ceased its characteristic voltage and calcium influx activity after 20 seconds, whereas the 40 day-old organoid kept a consistent beating rate throughout the experiment (**Figure 7**).

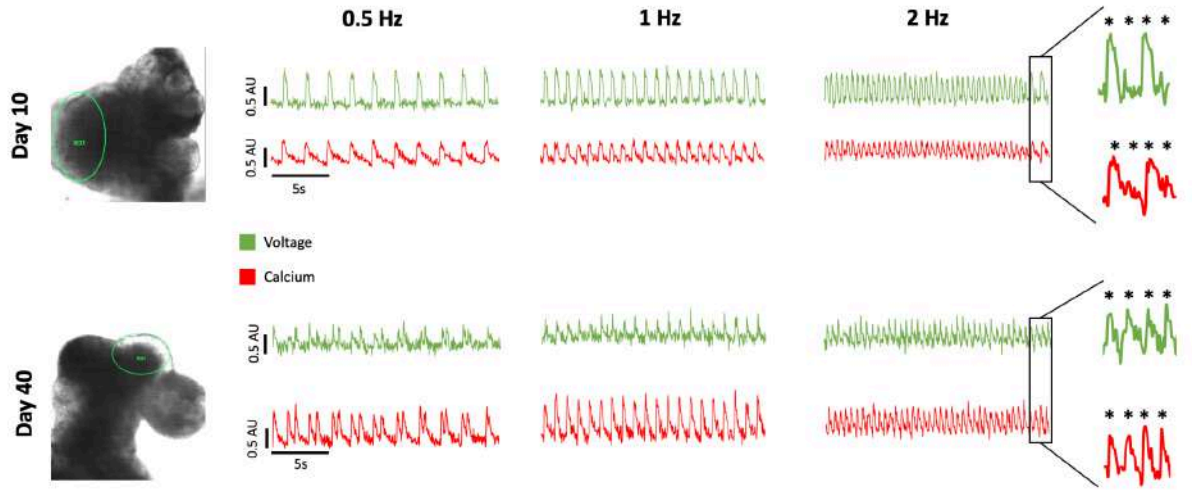

Figure 7. Comparison of induced electrical activity. In 10 and 40-day old organoids (*n*=2), a region of interest (ROI) was delineated based on the maximal detection of electrophysiological activity in a 20 seconds time frame. Two different cardiac organoids were tested, at 0.5, 1, and 2 Hz. In the 2 Hz group, after 20 seconds of electrical activity, the 10 days-old organoids stopped their usual voltage and calcium entrance activity after 20 seconds of the experiment in comparison to the 40 days-old cardiac organoids. Asterisks are used to compare Abbreviations: AU: arbitrary unit, S: seconds.

Compound treatments comparison

Gene expression analysis of compound groups

Cardiac organoids presented a significant expression of different cardiac-specific genes (**Figure 8**). Gene expression across molecular markers did not differ across different conditions; conversely, the ventricular marker *MYH7* presented higher expression in the reference control group (tto 2) compared to the carrier group (tto 1). Despite tto 2 not acting as the main reference for conditions, the 10 mM PA group (tto 3), and the combination of 2.25 mM PA and HG (tto 6) also showed significant differences with this reference group. Cq expression across the compound groups exhibited a range of 23 to 30 revealing high expression in the different markers.

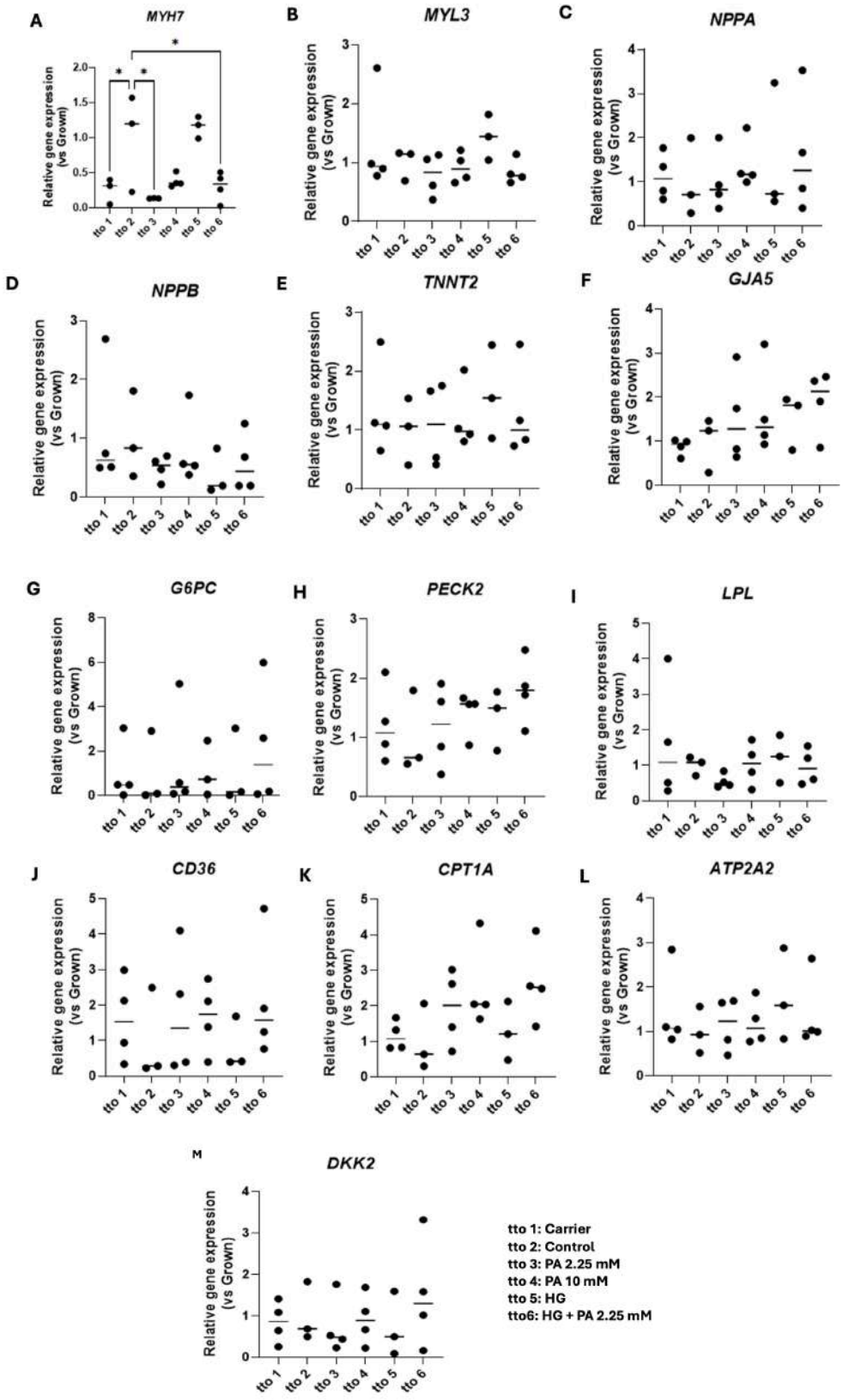

Figure 8. Gene expression over the different compound treatments. Graphical representation of the different genes measured in four independent cardiac organoid batches (*n*=3-4 organoids from each batch). Relative gene expression of: **A)** *MYH7* (Cq= 29.0), **B)** *MYL3* (Cq= 24.5), **C)** *NPPA* (Cq= 23.9), **D)** *NPPB* (Cq= 29.7), **E)** *TNNT2* (Cq= 23.6), **F)** *GJA5* (Cq= 27.7), **G)** *G6PC* (Cq= 29.7), **H)** *PECK2* (Cq= 29.2), **I)** *LPL* (Cq= 29.1), **J)** *CD36* (Cq= 29.4), **K)** *CPT1A* (Cp= 28.9), **L)** *ATP2A2* (Cq= 23.2) and **M)** *DKK2* (Cq= 30.2). Abbreviations: Cq: quantification cycle. HG: high glucose. PA: palmitic acid. tto: treatment. * *P* ≤0.05 vs control reference group (tto 2).

Size and internal complexity of cardiac organoid cells

Forward Side-scatter Cell (FSC)

While comparing cell size (FSC), there was a statistically significant difference between the reference control group (tto 2) and 10 mM PA treated group (tto 4), with a decrease in FSC from tto 4 in comparison to tto 2 (360.7 ± 10.10 vs. 381.4 ± 4.62); *P* <0.032). Similarly, there was a statistically significant difference between high glucose (tto 5) in comparison to control (tto 2) (347.9 ± 2.44 vs. 381.4 ± 4.62; *P* <0.0004) (**Figure 9**).

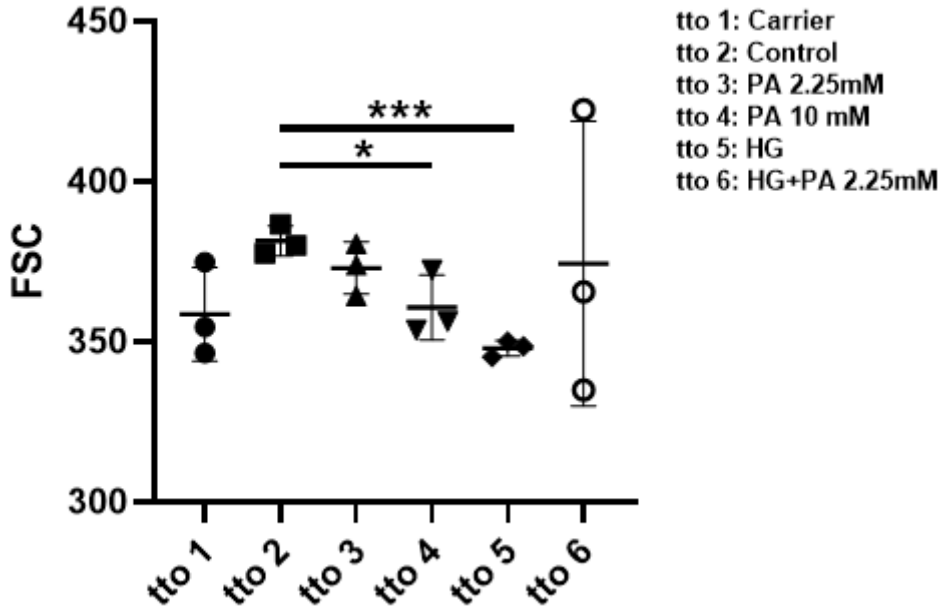

Figure 9. Graphical representation of cell size from different compound groups. Forward-side scatter cell (FSC) quantification was used on flow cytometry to determine cell size values within different compound groups (*n* = 3) after the induction of diabetic conditions had been completed. Abbreviations: PA: palmitic acid; tto: treatment; HG: high glucose. **P* <0.032, ****P* <0.0004 vs control reference group (tto 2).

Side-scatter Cell (SSC) internal complexity of a cell

There was a statistically significant difference between the reference control group (tto 2) and high glucose group (tto 5), with a decrease in the granularity of group 5 in comparison to the control (186.6 ± 25.84 vs 124.6 ± 28.74; *P* <0.048) (**Figure 10**).

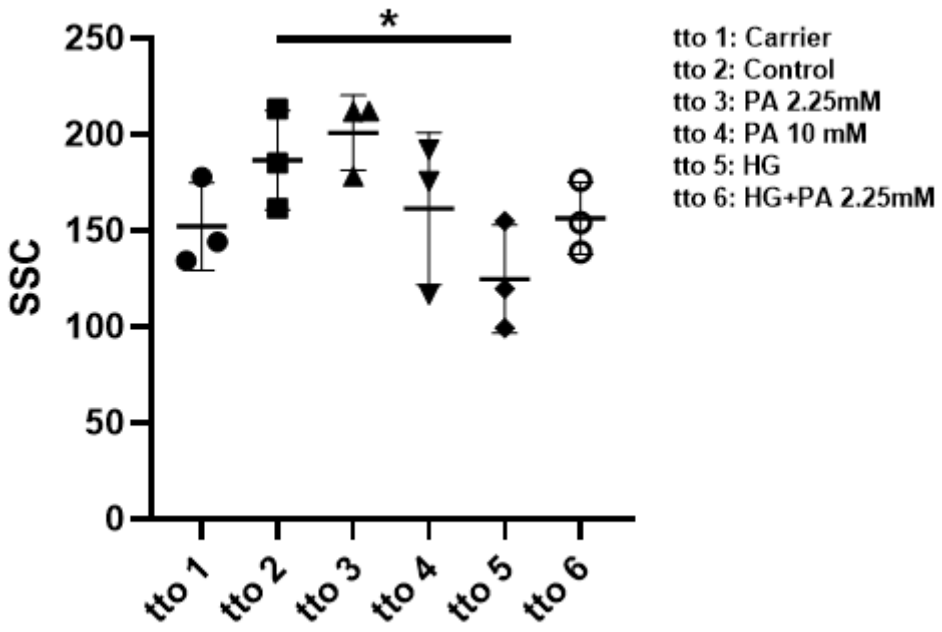

Figure 10. Graphical representation of granularity from different compound groups. Side-scatter Cell (SSC) quantification was used on flow cytometry to determine granularity values from each compound group (*n*=3) once the induction of diabetic conditions had finished. Abbreviations: PA: palmitic acid; tto: treatment; HG: high glucose. **P* <0.048 vs control reference group (tto 2).

DISCUSSION

Human cardiac organoids provide complex *in vitro* mini hearts that accurately reproduce some of the physiological and developmental features of the human heart. Actually, this approach can also be suitable for studying the mechanisms of disease and the impact of therapies in various pathological conditions, including diabetes. One of the primary objectives of this study was to establish the optimal conditions in our laboratory for generating cardiac organoids from induced pluripotent stem cells (iPSCs). Functional and gene expression analysis of cardiac organoids revealed that the differentiation procedures used were successful. Indeed, our cardiac organoids not only expressed cardiac-specific biomarkers but also responded to different electrical and beta-adrenergic-mediated stimuli. On the other hand, we also aimed to investigate the contribution of diabetic conditions to cardiac organoid physiology and remodeling by assessing the expression of a select set of molecular targets. The majority of gene expression analysis did not reveal noticeable changes among the experimental conditions, except for *MYH7* when compared to the reference group. However, both cell size and internal complexity (granularity) were lower in cardiac organoids treated with high glucose compared to those of the control organoids.

The development of cardiac organoids derived from iPSCs has been beneficial for mimicking heart development from less differentiated stages to advanced mature stages. As previously described (Volmert and Aguirre, 2024), the analysis of cardiac organoids at day 23 was established as an early stage of development, i.e., at the starting point of the maturation period, whereas the second time point took place on day 35, once the maturation period was completed. This allowed for the evaluation of maturation success based on mRNA expression, with expectedly higher values compared to the earlier stage. The final sample collection was performed on day 41. Additionally, organoids displayed upregulation in different genes, as described by Aguirre et al., these changes indicate an important growth and remodeling process even after day 34 of differentiation.

Regarding the first part of this study, one of the main findings was the expression of cardiac and metabolic molecular targets in differentiated cardiac organoids, regardless of their state of differentiation; however, the gene expression rate exhibited by the different molecular markers used did not significantly differ between early and advanced stages. This could be at least in part attributed to the short period of time between the early and mature stages of cardiac organoids that were considered for the molecular and functional analysis. According to gene expression analysis, the quantitative cycle (Cq) values ranged from 23 to 30, indicating robust and reliable expression for the different gene probes used in the study, which further confirmed overall optimal transcriptional activity within the cardiac organoids at these developmental stages. Likely, both the molecular and functional changes could have been higher if earlier stages of differentiation had been used. Despite this, the presence of detectable levels of cardiac-specific markers also uncovered anatomical differentiation given by the retrieved values, although our analyses did not allow us to identify specific compartmental zones within each anatomical structure.

Another important observation was the induction of a consistent and stable beating rate (as revealed by either the cycles of Ca2+ release and entry or electrophysiological response to external electrical stimulation over time) at advanced stages of cardiac organoid differentiation. Indeed, our data revealed that the beating rate was higher in advanced stages of differentiation. A proper electrical maturation is a crucial step in assessing cardiac development and functionality, since the beating of the organoids is secondary to an electrical signal emerging within them, and not because of external stimuli. We demonstrated that organoids from different maturation stages (10 and 40 days) exhibit a peak in voltage amplitude, which corresponds to calcium entry into the membrane. These results indicate that the beating of the organoids is not due to a simple incidental effect, but is secondary to an electrical activity, which is similar to that of a physiological heart. Moreover, the cardiomyocytes possessed ventricular-, atrial- and nodal-like action potentials; in the human heart, the cardiac action potential is the driving force for contraction and

functionality. As such, this opens the door for future electrical applications, disease modeling, or drug testing. The comparison between amplitude action/potential (AP) and calcium entrance with normalized change in fluorescence intensity, was determined using the fitted mixed-effect model, since this is far more flexible for complex experimental designs, including those with multiple sources of variation, varying numbers of repeated measures per subject, and continuous predictors and allows for inferences about both the specific groups studied (fixed effects) and the broader population from which random effects were sampled (in comparison to ANOVA). There was a statistically significant difference between 100 mM isoproterenol and the stage of development of the cardiac organoids in contrast with AP amplitude; in the 40 days-old organoid, there is a decrease in the AP amplitude activity, which can be due to the use of Fluovolt™ Dye, which is a fluorophore whose properties with isoproterenol are not fully understood. The inotropic effect persists on day 40 cardiac organoid, and there is no longer a significant difference between the control and iso compared to day 10 cardiac organoid, finally, the inotropic effect is related to the calcium signal. Remarkably, the mature cardiac organoids exhibited an enhanced capability to respond to both voltage-induced and beta-adrenergic-mediated stimuli compared to that of less-differentiated organoids. Unfortunately, this type of functional analysis was not assessed in earlier differentiation stages of cardiac organoids. Regarding cardiac-specific molecular targets and functional analysis, our data align with the findings reported by Aguirre *et al*., Both studies consistently demonstrate a progressive advancement in electrical activity, corresponding with the maturation stage of the organoids. Our investigation into gene expression revealed a significant correlation between two distinct developmental stages, an observation that expands upon previous research, which focused on a singular time point during development. Notably, this analysis of metabolism-related genes across both developmental stages demonstrated detectable expression levels of metabolic targets, even before the full maturation stage was achieved.

The second part of the study was focused on mRNA analysis of the same molecular targets under induced diabetic conditions at an advanced development stage, specifically when cultured cardiac organoids had completed their primary growth phase and all growth-promoting supplements had been withdrawn. Our data did not reveal significant changes in the gene expression of cardiac-specific or metabolic-related markers in cardiac organoids. Gene expression analysis was set to evaluate the effects of high glucose and PA in cardiac organoids. Because PA is formulated by mixing with BSA, the first set of analyses included ruling out a potential impact of BSA treatment (tto 1) on gene expression and then comparing PA-treated groups with their BSA carrier reference. The second set of analysis focused on comparing the control group (tto 2) with the HG group (tto 5). This

comparison focused on eliminating potential bias by assessing baseline gene expression in the absence of PA, relative to the continued maturation environment.

A statistically significant difference was observed only in the expression of *MYH7*, a ventricular marker found in these organoid models. Specifically, when comparing the reference control group (tto 2) with the carrier group, 2.25 mM PA and HG+2.25 mM PA showed a downregulated expression of *MYH7* in cardiac organoid groups treated with PA. Conversely, the primary comparison between carriers and groups where PA was used revealed that the addition of PA did not modify gene expression in such groups. However, this finding may be secondary to the sustained presence of maturation medium in the control group, which likely promoted the development of larger ventricular compartments within the cardiac organoids (ventricles typically exhibit higher *MYH7* expression). In contrast, the groups treated with PA may have experienced malformations or signs of cardiac injury as a consequence of this fatty acid, leading to a comparatively lower *MYH7* expression.

Furthermore, we showed that the organoids that achieved the second maturation stage can be used as models for investigating the use of HG and PA in mimicking DCM. Increased levels of PA have been described to mimic diabetic conditions in endothelial progenitor cells (Trombetta *et al.*, 2013), it was found that doses greater than or equal to PA 300 µmol/L caused a genetic change in these cells. Since it had not been tested in cardiac organoids, this concentration was taken as a starting point and two groups of increased PA concentrations were created, since this was a research model where the appropriate concentrations to mimic DCM are not yet described, 2.25 mM of PA could resemble the diabetic conditions in humans, whilst 10 mM was used to metabolically force these organoids to assess its impact on cell size and gene expression differences. Regarding increased glucose concentration, a protocol previously described the amount needed to mimic these diabetic conditions in cardiac organoids, since 11.1 mM or more are considered diabetic in humans (Lewis-Israeli *et al.*, 2022).

Among metabolic genes, our data showed that the expression of none of them was significantly influenced by the established diabetic conditions. In particular, the expression of metabolic sensors of carbohydrate (i.e., *G6PC* and *PCK2*) (Yu *et al.*, 2021), nor fatty acid uptake (i.e., *CD36*) (Li *et al.*, 2022); (Ke *et al.*, 2023), which are upregulated by insulin resistance in cardiac tissue, did not differ among groups. The result was directly due to the high dispersion of each gene expression value, which at least in part could be attributed to the small number of independent replicates. Possibly, the analysis of protein abundance, a better correlate of function, rather than gene expression might be more informative. Unfortunately, we could not reach assessing the functional assays to confirm this.

Flow cytometry analysis revealed that cardiac organoids exposed to high glucose concentrations exhibited a significant decrease in both cell size and internal complexity (granularity) compared to control organoids. This reduction is likely due to glucose induced cellular damage. The accumulation of glucose can harm cellular components, leading to atrophy. Furthermore, as a protective mechanism against severe damage, some cells may undergo apoptosis, which could account for the observed decrease in granularity. Although apoptosis was not evaluated in this experiment, it should be performed in further studies.

For future evaluation, increasing the sample size is crucial. A larger number of cardiac organoids will enhance the statistical precision of the results and yield more significant mean values. Regarding RNA extraction, it is recommended to explore the use of different kits. In this study, using a single kit resulted in low RNA values, as measured by Nanodrop 2000 Spectrophotometer, suggesting that optimizing the extraction method could significantly improve RNA quantity and quality for downstream analyses. Furthermore, a pool of three to four organoids must be sufficient to obtain a higher RNA value.

To sum up, future research should focus on identifying and testing reversal treatments for the observed DCM effects. Additionally, incorporating microscopic analysis of ethanol-fixed organoid sections will enable a detailed examination of their anatomical structure, allowing for differentiation between them. While the tested genes provided information regarding anatomical structures and various metabolic processes, it is recommended that further studies analyze inflammation markers in the use of these models with DM conditions, as many cytokines and chemokines are released in the pathophysiology of T2D.

CONCLUSIONS

As a conclusion to the first part of the study, our gene expression and functional data demonstrate that we achieved functional cardiac organoids expressing cardiac-specific markers. Although the analysis of morphological complexity was lacking, we unveiled nodes and a more advanced state of electrophysiological maturation when compared to those found in the growing stage.

Moreover, as a conclusion from the second part of the study, our data did not reveal significant changes in the gene expression of cardiac-specific nor metabolic-related markers in cardiac organoids, at least in part due to the overall high variability in their gene expression rate across different batches.

REFERENCES

-American Diabetes Association Professional Practice Committee (2024). Standards of Care in Diabetes-2024. Diabetes Care 47.

-Boudina, S. and Abel, E.D. (2007) 'Diabetic Cardiomyopathy Revisited', *Circulation*, 115(25), pp. 3213–3223. Available at: https://doi.org/10.1161/CIRCULATIONAHA.106.679597.

-Boudina, S. and Abel, E.D. (2010) 'Diabetic cardiomyopathy, causes and effects', *Reviews in Endocrine and Metabolic Disorders*, 11(1), pp. 31–39. Available at: https://doi.org/10.1007/s11154-010-9131-7.

-Corrò, C., Novellasdemunt, L. and Li, V.S.W. (2020) 'A brief history of organoids', *American Journal of Physiology-Cell Physiology*, 319(1), pp. C151–C165. Available at: https://doi.org/10.1152/ajpcell.00120.2020.

-Drakhlis, L. *et al.* (2021) 'Human heart-forming organoids recapitulate early heart and foregut development', *Nature Biotechnology*, 39(6), pp. 737–746. Available at: https://doi.org/10.1038/s41587-021-00815-9.

-Evans, M.J. and Kaufman, M.H. (1981) 'Establishment in culture of pluripotential cells from mouse embryos', *Nature*, 292(5819), pp. 154–156. Available at: https://doi.org/10.1038/292154a0.

-Fan, X.-L. *et al.* (2020) 'Mechanisms underlying the protective effects of mesenchymal stem cell-based therapy', *Cellular and Molecular Life Sciences*, 77(14), pp. 2771–2794. Available at: https://doi.org/10.1007/s00018-020-03454-6.

-Hofbauer, P. *et al.* (2021) 'Cardioids reveal self-organizing principles of human cardiogenesis', *Cell*, 184(12), pp. 3299-3317.e22. Available at: https://doi.org/10.1016/j.cell.2021.04.034.

-Jia, G., Hill, M.A. and Sowers, J.R. (2018) 'Diabetic Cardiomyopathy: An Update of Mechanisms Contributing to This Clinical Entity', *Circulation Research*, 122(4), pp. 624–638. Available at: https://doi.org/10.1161/CIRCRESAHA.117.311586.

-Jo, J. *et al.* (2016) 'Midbrain-like Organoids from Human Pluripotent Stem Cells Contain Functional Dopaminergic and Neuromelanin-Producing Neurons', *Cell Stem Cell*, 19(2), pp. 248–257. Available at: https://doi.org/10.1016/j.stem.2016.07.005.

-Kanisicak, O. *et al.* (2016) 'Genetic lineage tracing defines myofibroblast origin and function in the injured heart', *Nature Communications*, 7(1), p. 12260. Available at: https://doi.org/10.1038/ncomms12260.

-Ke, J. *et al.* (2023) 'Diabetic cardiomyopathy: a brief summary on lipid toxicity', *ESC Heart Failure*, 10(2), pp. 776–790. Available at: https://doi.org/10.1002/ehf2.14224.

-Lewis‐Israeli, Y.R. *et al.* (2022) 'Modeling the Effects of Maternal Diabetes on the Developing Human Heart Using Pluripotent Stem Cell–Derived Heart Organoids', *Current Protocols*, 2(6), p. e461. Available at: https://doi.org/10.1002/cpz1.461.

-Li, Y. *et al.* (2022) 'CD36 favours fat sensing and transport to govern lipid metabolism', *Progress in Lipid Research*, 88, p. 101193. Available at: https://doi.org/10.1016/j.plipres.2022.101193.

-Liu, C. *et al.* (2022) 'Generating 3D human cardiac constructs from pluripotent stem cells', *eBioMedicine*, 76, p. 103813. Available at: https://doi.org/10.1016/j.ebiom.2022.103813.

-Lu, X. *et al.* (2024) 'Type 2 diabetes mellitus in adults: pathogenesis, prevention and therapy', *Signal Transduction and Targeted Therapy*, 9(1), p. 262. Available at: https://doi.org/10.1038/s41392-024-01951-9.

-Mattapally, S. *et al.* (2018) 'Spheroids of cardiomyocytes derived from human-induced pluripotent stem cells improve recovery from myocardial injury in mice', *American Journal of Physiology-Heart and Circulatory Physiology*, 315(2), pp. H327–H339. Available at: https://doi.org/10.1152/ajpheart.00688.2017.

-Méndez-Lara, K.A. *et al.* (2018) 'Administration of CORM-2 inhibits diabetic neuropathy but does not reduce dyslipidemia in diabetic mice', *PLOS ONE*. Edited by M.C. Vinci, 13(10), p. e0204841. Available at: https://doi.org/10.1371/journal.pone.0204841.

-Ng, K.-M. *et al.* (2018) 'Empagliflozin Ameliorates High Glucose Induced-Cardiac Dysfunction in Human iPSC-Derived Cardiomyocytes', *Scientific Reports*, 8(1), p. 14872. Available at: https://doi.org/10.1038/s41598-018-33293-2.

-Nugraha, B., Buono, M.F. and Emmert, M.Y. (2018) 'Modelling human cardiac diseases with 3D organoid', *European Heart Journal*, 39(48), pp. 4234–4237. Available at: https://doi.org/10.1093/eurheartj/ehy765.

-Ong, K.L. *et al.* (2023) 'Global, regional, and national burden of diabetes from 1990 to 2021, with projections of prevalence to 2050: a systematic analysis for the Global Burden of Disease Study 2021', *The Lancet*, 402(10397), pp. 203–234. Available at: https://doi.org/10.1016/S0140-6736(23)01301-6.

-Riehle, C. and Bauersachs, J. (2019) 'Of mice and men: models and mechanisms of diabetic cardiomyopathy', *Basic Research in Cardiology*, 114(1), p. 2. Available at: https://doi.org/10.1007/s00395-018-0711-0.

-Stanley, W.C., Recchia, F.A. and Lopaschuk, G.D. (2005) 'Myocardial Substrate Metabolism in the Normal and Failing Heart', *Physiological Reviews*, 85(3), pp. 1093–1129. Available at: https://doi.org/10.1152/physrev.00006.2004.

-Trombetta, A. *et al.* (2013) 'Increase of Palmitic Acid Concentration Impairs Endothelial Progenitor Cell and Bone Marrow–Derived Progenitor Cell Bioavailability', *Diabetes*, 62(4), pp. 1245–1257. Available at: https://doi.org/10.2337/db12-0646.

-Volmert, B. and Aguirre, A. (2024) 'Methods for Generating Self-Organizing Human Patterned Heart Organoids Using Pluripotent Stem Cells', in. New York, NY: Springer US (Methods in Molecular Biology). Available at: https://doi.org/10.1007/7651_2024_545.

-Volmert, B. *et al.* (2023) 'A patterned human primitive heart organoid model generated by pluripotent stem cell self-organization', *Nature Communications*, 14(1), p. 8245. Available at: https://doi.org/10.1038/s41467-023-43999-1.

-Volpato, V. and Webber, C. (2020) 'Addressing variability in iPSC-derived models of human disease: guidelines to promote reproducibility', *Disease Models & Mechanisms*, 13(1), p. dmm042317. Available at: https://doi.org/10.1242/dmm.042317.

-Vos, T. *et al.* (2020) 'Global burden of 369 diseases and injuries in 204 countries and territories, 1990–2019: a systematic analysis for the Global Burden of Disease Study 2019', *The Lancet*, 396(10258), pp. 1204–1222. Available at: https://doi.org/10.1016/S0140-6736(20)30925-9.

-Weinberger, F., Mannhardt, I. and Eschenhagen, T. (2017) 'Engineering Cardiac Muscle Tissue: A Maturating Field of Research', *Circulation Research*, 120(9), pp. 1487–1500. Available at: https://doi.org/10.1161/CIRCRESAHA.117.310738.

-Yu, S. *et al.* (2021) 'Phosphoenolpyruvate carboxykinase in cell metabolism: Roles and mechanisms beyond gluconeogenesis', *Molecular Metabolism*, 53, p. 101257. Available at: https://doi.org/10.1016/j.molmet.2021.101257.